J Appl Electrochem (2011) 41:51–62
DOI 10.1007/s10800-010-0206-7

ORIGINAL PAPER

Electrochemical discolouration and degradation of reactive dichlorotriazine dyes: reaction pathways

Elzbieta Kusmierek · Ewa Chrzescijanska · Magdalena Szadkowska-Nicze · Joanna Kaluzna-Czaplinska

Received: 5 January 2010 / Accepted: 5 September 2010 / Published online: 17 September 2010

Abstract Results of electrochemical oxidation of two reactive dichlorotriazine dyes: Reactive Red 2 and Reactive Blue 81, are presented in this paper. Two electrode materials: Ti/TiO_2(70%)–RuO_2(30%) and carbon felt, were applied in the investigations as anodes. Voltammetric measurements show that Reactive Blue 81 electrooxidation proceeds easier and with higher rate than electrooxidation of Reactive Red 2. Both dyes are oxidised irreversibly in at least one electrode step before oxygen evolution starts at the electrode. Effectiveness of electrochemical oxidation under potentiostatic conditions achieved for Reactive Blue 81 was higher than for Reactive Red 2, with application of a carbon felt anode. Pulse radiolysis measurements prove addition of $^{\bullet}OH$ radical to the dye molecule and formation of cyclohexadienyl and naphthoxyl radicals. Results of voltammetric analysis, pulse radiolysis measurements and GC–MS identification of intermediate products suggest two possible pathways of the dyes electrochemical oxidation.

Keywords Electrochemical oxidation · Reactive dyes · Degradation products · Electrochemical degradation pathways

E. Kusmierek (✉) · E. Chrzescijanska · J. Kaluzna-Czaplinska
Institute of General and Ecological Chemistry,
Technical University of Lodz, ul. Zeromskiego 116,
90-924 Lodz, Poland
e-mail: ekusmier@p.lodz.pl

M. Szadkowska-Nicze
Institute of Applied Radiation Chemistry,
Technical University of Lodz, ul. Wroblewskiego 15,
90-590 Lodz, Poland

1 Introduction

Dyes used in textile industry should be light resistant and should not fade during washing. Among azo dyes, reactive dyes are produced in large amounts and released to the environment during dyeing process. Azo type reactive dyes are resistant to biological degradation under aerobic conditions [1, 2]. Anaerobic treatment should not be applied because breakdown of azo dye can result in formation of aromatic amines which are more toxic than the dye molecule [3, 4].

Several wastewater treatment methods, including physical, chemical and biological methods, were applied and resulted in total discolouration which does not imply total mineralization [5]. Electrochemical techniques seem to be an interesting alternative to commonly used treatment methods. These techniques have advantages and drawbacks. They use electrons as the main reagent; however, the presence of supporting electrolytes is required. Generally, the wastewater contains the supporting electrolyte, but its concentration is often not sufficient [4]. Electrochemical removal of organics can be achieved by an application of direct or indirect electrooxidation [6]. Direct electrooxidation results in transformation of organics to CO_2 and H_2O but is very slow and electrical charge required per molecule of organic species is very high [7]. Moreover, it is difficult to find cheap and inert electrode material. On the other hand, electrochemical processes require ambient temperature, lower than their equivalent non-electrochemical counterparts, without a need for temperature control [8, 9]. Direct electrochemical processes are often described as *electrochemical incineration* (ECI) if the degradation products are the same as in the case of thermal incineration, i.e., CO_2 [10]. ECI includes transfer of O-atoms from H_2O to oxidation products, but commonly

used anode materials, e.g., Au, Pt or glassy carbon, show slow heterogeneous kinetics in this process.

Dyes can be destroyed by direct and/or indirect oxidation. These processes are carried out with oxidants such as hydroxyl radicals, ozone and hypochlorite ions [11]. The oxidation rate, its mechanism and products of anodic reaction depend strongly on the material of the anode. Rate removal of organics is higher if anodes with high oxygen overvoltage are applied [12]. Otherwise, a large part of electrical charge is used to produce oxygen [13]. Boron-doped diamond (BDD) and metal oxide anodes show high O_2 evolution overpotential, and generation of hydroxyl radicals ($^{\bullet}OH$) at their surface was proved during electrolytic catalytic process [13–16]. Hydroxyl radicals are generated from the oxidation of water and their lifetime is very short (only few nanoseconds) [17]. They are strongly oxidizing species due to their high oxidation potential ($E^0 = 2.80$ V) and can completely degrade organic molecules.

Electrochemical degradation of different textile dyes was reported at various electrode materials [18, 19]. Commonly used electrodes such as graphite, platinum and dimensionally stable anodes (DSA®) do not show sufficient O_2 evolution overpotential. This drawback does not concern currently available PbO_2, SnO_2, TiO_2 and diamond electrodes [4, 20–23]. High-overpotential metal oxides anodes for oxygen evolution are relatively cheap and easy to manufacture. Nanostructured semiconductor thin-film electrodes of Ti/TiO_2 are characterized by electrochemical stability and large internal surface areas which results in higher efficiency during degradation of organic compounds [24–27].

Reactive dyes are the main group of dyes used in dyeing of cellulose fibres. Only 60–90% of reactive dyes are effectively used in the dyeing process [28]. Consequently, a significant amount of unfixed dyes is released to wastewater. Concentrations of reactive dyes in the industrial wastewater vary from 5 to 1500 mg L^{-1} [29].

The aim of this work was to study the electrochemical discolouration and degradation of reactive dichlorotriazine dyes. Two reactive dyes: Reactive Red 2 (RR2) and Reactive Blue 81 (RB81) were selected as model compounds because they are commonly used in the textile industry. Their discolouration and degradation was investigated in aqueous solutions under potentiostatic conditions, with the application of two different anode materials: $Ti/TiO_2(70\%)$–$RuO_2(30\%)$ and carbon felt (WRW5). Differences in the electrochemical behaviour of these materials was found out by cyclic voltammetry measurements. The efficiency of the reactive dyes discolouration and degradation was estimated by changes in absorption spectra as well as TOC and COD removal. Products of the first step of electrochemical oxidation at titanium electrode covered with titanium and ruthenium oxides were determined by GC–MS analysis. Molecules of reactive dyes investigated in this work are relatively large, thus several products can be expected during their electrooxidation. For prediction of the possible pathways of the electrochemical oxidation: direct and indirect by hydroxyl radicals, products analysis, quantum-chemical calculations and the pulse and steady-state radiolysis of dyes aqueous solutions were performed. The results obtained will help to select the most suitable electrode material for electrochemical degradation of reactive dyes and could be the basis for development of the degradation method on an industrial scale.

2 Materials and methods

2.1 Chemicals

The subject of the investigation was RR2 (Reactive Red 2, Helaktyn Red F5B, C.I. 18 200) and RB81 (Reactive Blue 81, Helaktyn Blue F2R, C.I, 18 245) obtained from Dyestuff Industry Works Boruta S.A. in Zgierz—Poland. These dyes are anionic and water soluble. They give good colour fastness due to the presence of the reactive system—dichlorotriazine group. Helaktyn dyes are designed for dyeing and printing of cellulosic, protein and polyamide fibers. These dichlorotriazine dyes are applied in dyeing with exhaust method at low temperatures ranging from 25 to 45 °C and for semicontinuous method, called pad-batch. Absorption spectra of the dyes and their structures are presented in Fig. 1.

Within the visible region (380–780 nm), absorption bands are observed at the wavelength of 536 and 584 nm for RR2 and RB81, respectively. They correspond to the π–π^* transition of electrons in the azo-group connecting

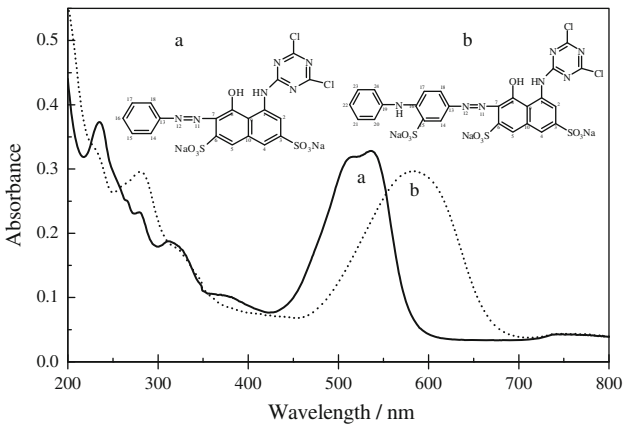

Fig. 1 Absorption spectra and structures of RR2 (*a*) and RB81 (*b*); $c = 10^{-5}$ mol L^{-1}, $l = 1$ cm, $\varepsilon_{RR2} = 3.3 \times 10^4$ ($\lambda = 536$ nm), $\varepsilon_{RB81} = 3.0 \times 10^4$ ($\lambda = 584$ nm)

phenyl and naphtyl. A decrease in the absorbances at these wavelengths is connected with the discolouration of the dye solution. Within near ultraviolet region (280–380 nm), absorption bands result from the unsaturated system of benzene and naphthalene ring [30]. Decrease in the absorbances at this wavelength range indicates mineralization of the dye.

The aqueous solutions of dyes, used in electrochemical investigations, were prepared by dissolution of the dye in 0.1 mol L^{-1} $NaClO_4$ ($NaClO_4 \cdot H_2O$, Fluka). The concentration of the dye solution used in experiments was 0.5 g L^{-1}. For the radiolysis experiments, the dyes were purified by double recrystallization from ethanol (70%)–water (30%) mixtures, and solutions were prepared using reagent-grade water from a Millipore Milli-Q system. These solutions were deoxygenated by bubbling with nitrous oxide (N_2O) in order to obtain oxidizing medium.

In GC–MS analyses, the following chemicals: water (Labscan for HPLC) and diethyl ether (POCH SA for HPLC) were used. All other chemicals used in the experiments were of analytical pure grade and were used without further purification.

2.2 Electrodes

The following electrodes were used in the investigation: titanium covered with titanium and ruthenium oxides and carbon felt. Titanium electrode covered with titanium (70%) and ruthenium (30%) oxides (Ti/TiO_2(70%)–RuO_2(30%)) was prepared in the process which involved thermal decomposition of ruthenium and titanium chloride spread on a appropriately prepared titanium base. Carbon felt in the form of a cloth was obtained from Carbon Electrodes Plant in Raciborz—Poland. Its specific surface was 2.5 m^2 g^{-1}. All electrodes had a geometric area of 2 or 20 cm^2 exposed to the solution in the voltammetric experiments and electrolysis, respectively. Platinum electrode in the form of a sheet was used as a cathode. Saturated calomel electrode (SCE) was applied as a reference electrode.

2.3 Experimental procedure

2.3.1 Electrolysis

A preparative oxidation of the dyes under potentiostatic conditions was carried out in an electrochemical cell with divided electrode compartments. Anode potential was controlled versus SCE. Ti/TiO_2(70%)–RuO_2(30%) and carbon felt was applied as an anode material. Platinum sheet was used as a cathode. Anode and cathode surface was 20 cm^2.

Electrolyses were carried out in the anode potential range from 0.7 to 2.0 V. Several electrolyses were carried out under galvanostatic conditions for 2 h and at the current density of 0.02 A cm^{-2}. Volume of dyes solutions electrolysed was 60 mL. Concentration of dyes was 0.5 g L^{-1}. The supporting electrolyte was 0.1 mol L^{-1} $NaClO_4$.

2.3.2 Radiolysis

Radiolysis studies were carried out with high energy (6 MeV) electron pulses generated by linear electron accelerator ELU-6 (USSR made). 17 ns electron pulses (dose ca. 55 Gy) and 4 μs pulses (dose ca. 0.8 kGy) were used for the pulse and steady-state radiolysis experiments, respectively. The dose absorbed per pulse was determined with N_2O saturated aqueous solution of KSCN (0.01 mol L^{-1}), assuming $G((SCN)_2^{\bullet -}) = 6.0$ and $\varepsilon((SCN)_2^{\bullet -}) = 7600$ dm^3 mol^{-1} cm^{-1} (G represents yield of radicals per 100 eV of energy absorbed and ε is a molar extinction coefficient at 475 nm). More details concerning detection system and the accelerator can be found in [31]. Solutions of the dyes (ca. 3 mL in volume) were irradiated in a Spectrosil A rectangular cells with optical path length of 1 cm. In steady-state experiments the optical absorption spectra were recorded 5 min after the end of irradiation using a Cary 5E spectrophotometer (Varian Ltd.). The concentration of a dye was kept in the range of 6–8 × 10^{-5} mol L^{-1}. Before irradiation, the dyes solutions were saturated with N_2O for 30 min in order to convert solvated electrons (e_{aq}^-), generated during radiolysis, to $^{\bullet}OH$ radicals.

2.4 Analytical methods

2.4.1 Voltammetric analysis

The investigation was carried out in a three-electrode cell using cyclic voltammetry. Voltammetric curves were recorded with an Autolab electroanalytical set (Ecochemie, Holland). Dependence of current on the potential of the working electrode in the electrooxidation of reactive dyes was determined. Potential of the working electrode was measured versus SCE. Ti/TiO_2(70%)–RuO_2(30%) and carbon felt with surface area of 2 cm^2 was used as the anode. Platinum was used as an auxiliary electrode. The solutions were deoxygenated by purging with argon prior to the measurements. During the measurements, a blanket of argon was kept over the solutions. The volume of dyes solutions used in measurements was 15 mL. Concentration of both dyes solutions was 0.5 g L^{-1} (0.1 mol L^{-1} $NaClO_4$).

2.4.2 GC–MS analysis

Gas-chromatography coupled with mass spectrometry (GC–MS) was used for the identification of dyes electrooxidation products. Samples of the dyes solutions after the electrooxidation, were collected, extracted and concentrated by solid phase extraction SPE (Strata C18-E, Phenomenex, 500 mg/3 mL). Next, they passed through the SPE column and were washed with water (1 mL) and eluted with diethyl ether (1 mL). Eluents were collected and analyzed in GC/MS system.

Analyses were carried out in the gas chromatograph (Agilent Technologies 6890N Network GC) coupled with a mass detector (5973 Network Mass Selective Detector) equipped with 70-eV electron impact (EI) mode. Analytes were separated in GC using an Agilent HP-5MS capillary column (30.0 m × 0.25 mm × 0.25 μm). The temperature program began at 50 °C and increased at the rate of 6 °C min^{-1} up to 280 °C with holding time of 1 min for each increment. Helium was used as carrier gas with a flow rate of 1.0 mL min^{-1}. Detection in MS followed the separation. A sample of 1 μL volume was injected in the splitless mode. The temperature of MS transfer line and source was 280 and 230 °C, respectively. The MS quadrupole temperature was 150 °C. The MS was equipped with electron ionization source (70 eV). The qualitative analysis was carried out under full-scan acquisition mode. The intermediate products were identified by comparing the mass spectra with standard spectra stored in NIST 98 Library.

2.4.3 Electrochemical degradation effectiveness

The effectiveness of the electrochemical process was determined as a conversion of the substrate calculated as a change in the chemical oxygen demand (COD), total organic carbon (TOC) and absorbances in UV–VIS spectra. TOC was analyzed with TOC 505A Shimadzu Total Organic Carbon Analyser. UV–VIS spectra were recorded in the wavelength range from 190 to 800 nm using UV–VIS spectrophotometer (Shimadzu UV-24001 PC). The solution samples were diluted five times prior to spectrophotometric measurements.

3 Results and discussion

3.1 Cyclic voltammograms of RR2 and RB81 oxidation

Electrochemical oxidation of RR2 and RB81 was studied at Ti/TiO_2(70%)–RuO_2(30%) and carbon felt electrode used as an anode. Figures 2 and 3 show voltammetric response of these dyes as a dependence of electrode reaction current on electrode potential.

Voltammetric measurements prove that electrochemical oxidation of RR2 and RB81 is an irreversible reaction and proceeds in at least one electrode step in the potential range lower than the potential at which oxygen evolution starts at the applied electrodes. The electrooxidation at Ti/TiO_2(70%)–RuO_2(30%) proceeds easier than at the carbon felt electrode for both dyes. The process performed at Ti/TiO_2(70%)–RuO_2(30%) starts at the potential of 0.65 and 0.42 V in the case of RR2 (Fig. 2) and RB81 (Fig. 3), respectively. In the case of carbon felt applied as an anode material, the electrooxidation of RR2 and RB81 starts from the potential of 0.8 and 0.5 V, respectively. In the potential range where a peak related to the dye electrooxidation is formed, dependence of the peak current on the square root of the scan rate is linear and crosses the origin of the coordinates. This proves two facts: lack of adsorption in this potential range and the diffusion control of the electrode process. Thus, the kinetic parameters of the first step

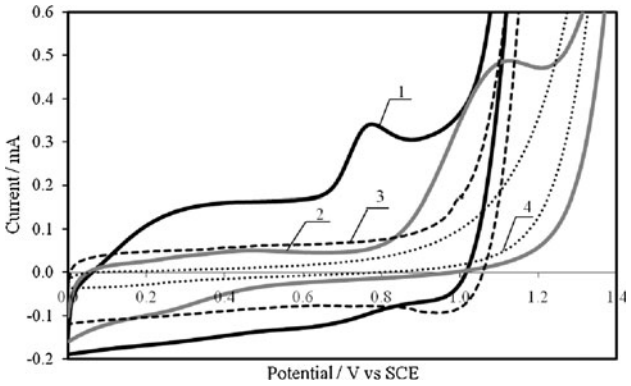

Fig. 2 Cyclic voltammograms recorded in the solution of RR2; *curve 1* Ti/TiO_2(70%)–RuO_2(30%), *2* carbon felt, and in the supporting electrolyte (0.1 mol L^{-1} $NaClO_4$); *curve 3* Ti/TiO_2(70%)–RuO_2(30%), *4* carbon felt; v = 0.01 V s^{-1}

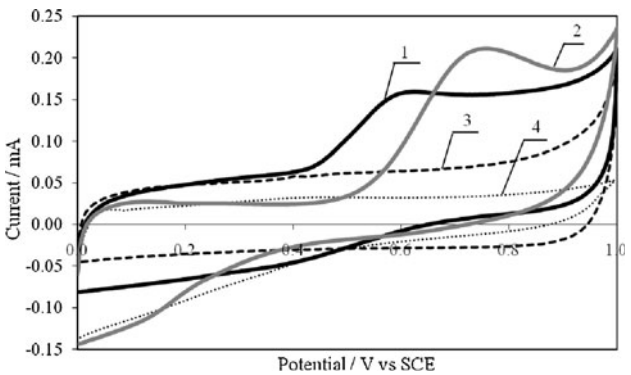

Fig. 3 Cyclic voltammograms recorded in the solution of RB81; *curve 1* Ti/TiO_2(70%)–RuO_2(30%), *2* carbon felt, and in the supporting electrolyte (0.1 mol L^{-1} $NaClO_4$); *curve 3* Ti/TiO_2(70%)–RuO_2(30%), *4* carbon felt; v = 0.01 V s^{-1}

Table 1 Values of peak potential (E_p), half-wave potential ($E_{1/2}$), anodic transfer coefficient (βn_β) and heterogeneous rate constant of the first step in the dyes electrooxidation at both electrode materials; $c = 500$ mg L^{-1} in 0.1 mol L^{-1} $NaClO_4$, $v = 0.01$ V s^{-1}, $D = 3 \times 10^{-6}$ cm^2 s^{-1}

Electrode material	E_p (V)	$E_{1/2}$ (V)	βn_β	k_{bh} at $E_{1/2}$ (cm s^{-1})
RR2				
Ti/TiO_2(70%)–RuO_2(30%)	0.80	0.73	0.50	0.15×10^{-3}
Carbon felt	1.10	1.04	0.30	0.12×10^{-3}
RB81				
Ti/TiO_2(70%)–RuO_2(30%)	0.60	0.56	0.45	0.20×10^{-3}
Carbon felt	0.76	0.67	0.40	0.14×10^{-3}

of the dyes electrooxidation at the investigated electrode materials were calculated (Table 1).

Peak potential (E_p) and half-wave potential ($E_{1/2}$) were determined by analyzing voltammograms recorded under linear diffusion conditions. The electron-transfer coefficient (βn_β) characterizes symmetry of the activated barrier of an electrode reaction. In order to compare the reaction rate at both electrode materials, the heterogeneous rate constant (k_{bh}) was determined at the half-wave potential [32].

The results show that RB81 is oxidized easier and at a higher rate than RR2. Both dyes are oxidized easier at the Ti/TiO_2(70%)–RuO_2(30%) electrode than at the carbon felt. The half-wave potentials of the dyes electrooxidation are about 0.15 V higher at the carbon felt.

These results were confirmed by quantum-chemical calculations of ionization potentials for both dyes made with AM1 method in HyperChem program. The ionization potential of RR2 totals 788.8 kJ mol^{-1} and is about 62.4 kJ mol^{-1} higher than in the case of RB81. This means that RB81 is easier oxidised than RR2.

3.2 Electrolyses under potentiostatic conditions

Electrolyses of the dyes solutions in the electrochemical cell with divided electrode compartments and under potentiostatic conditions were carried out in order to determine a possible pathway of the dyes electrooxidation. Anode potential varied from 0.6 to 2.0 V. Electrical charge passing through the electrochemical cell was constant during electrolyses (RB81—3.807 C, RR2—3.348 C) and corresponded to an exchange of two electrons. Example difference UV–VIS spectra of RB81 solutions from the anodic compartment are shown in Fig. 4. The y-axis in this figure presents Δabsorbances, i.e., a difference between absorbances recorded in the electrolysed solutions and absorbance in the dye initial solution. The Δabsorbances can have positive values if the absorbance of the

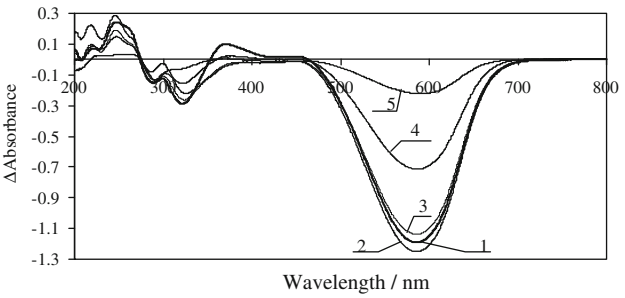

Fig. 4 Difference UV–VIS spectra of the RB81 solutions after the electrooxidation at various anode potentials with the application of Ti/TiO_2(70%)–RuO_2(30%); *curve 1* 0.6 V, *2* 0.7 V, *3* 0.9 V, *4* 1.0 V and *5* 1.2 V

intermediate product formed during the electrolysis, is higher at the given wavelength than the absorbance of the dye molecule which is decaying. The negative values of the Δabsorbances are observed only when a decrease in the absorbance at the given wavelength is caused by fading. One (RB81) or two (RR2) absorption bands are observed in the visible region of the spectra (Fig. 1). These bands are attributed to the transfer of electrons in the azo group present in the dye chromophore. Change in the absorbance within this region is connected with the discolouration of the dye solution. Within the near ultraviolet region, an absorption band, which can be attributed to a benzene ring, is observed at lower wavelengths than the band attributed to a naphthalene ring [33]. In the case of the RB81 electrooxidation at the Ti/TiO_2(70%)–RuO_2(30%) electrode, absorbances within the visible region decrease if the anode potential increases to 0.7 V. Further increase in the anode potential causes an increase in absorbances in this region. Moreover, changes in absorbances are very slight. The UV–VIS spectrum recorded for the RB81 solution after the electrooxidation at 0.6 V, shows one additional band of the absorption at the wavelength of 356 nm. This band can be attributed to the formation of cation-radical as the reaction product [34]. A decrease in the absorbance in the UV region proves mineralization of the dye solution.

The highest conversion degree of RB81 was reached during the electrolysis at the Ti/TiO_2(70%)–RuO_2(30%) anode potential of 0.9 V. Then, its conversion calculated as a change in TOC and COD was about 13 and 18% (Fig. 5), respectively. In absolute terms, the TOC values decreased from 60.1 ppm (RB81 initial solution) to 52.6 ppm (0.9 V) and next decreased to 58.5 ppm (1.2 V). In absolute terms, the COD values decreased from 191.2 mg L^{-1} (RB81 initial solution) to 155.9 mg L^{-1} (0.9 V) and next increased to 189.0 mg L^{-1} (1.2 V). When carbon felt was applied as the anode material, the best results were obtained during the electrolysis at the anode potential of 0.8 V. The RB81 conversion calculated as a change in TOC and COD was 20 and 32%, respectively. The TOC

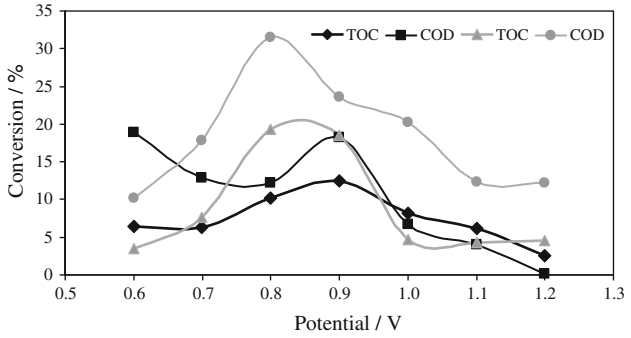

Fig. 5 Dependence of RB81conversion in the electrooxidation at Ti/TiO_2(70%)–RuO_2(30%) (▬) and carbon felt electrode (—), calculated as a change of TOC and COD, on the anode potential

and COD values in absolute terms deacreased from 60.3 ppm and 189.6 mg L^{-1} (RB81 initial solution) to 48.6 ppm and 129.9 mg L^{-1} (0.8 V), respectively. Further increase in the anode potential to 1.2 V caused the increase in TOC and COD values to 57.5 ppm and 166.4 mg L^{-1}, respectively. Moreover, duration of electrolyses was several times shorter than in the case of the Ti/TiO_2(70%)–RuO_2(30%) electrode. Assuming that at potentials higher than the peak potentials, electrooxidation proceeds with direct and indirect mechanism (higher contribution of the indirect mechanism), we can expect better results at Ti/TiO_2(70%)–RuO_2(30%) at potentials higher than the peak potential. This fact can be related to the amount of hydroxyl radicals formed at the electrodes and to contribution of the direct and indirect mechanism.

In the case of the RR2 electrooxidation in the electrochemical cell with divided electrode compartments and with the application of Ti/TiO_2(70%)–RuO_2(30%) electrode, changes in dyes conversion were similar to those observed for the RB81 dye. The highest dye conversion was obtained at the potential of 0.9 V. Its value calculated as the change in TOC and COD, was 14 and 39%, respectively. The TOC and COD values in absolute terms decreased from 64.6 ppm and 169.9 mg L^{-1} (RR2 initial solution) to 55.4 ppm and 103.6 mg L^{-1} (0.9 V), respectively. Absorbances within the visible region decrease with an increase in the potential above 0.9 V. However, changes in the absorbances within the ultraviolet region are slight. UV–VIS spectra recorded for the dye solution after the electrolysis at the potential of 0.6 V do not show any additional band at the wavelength of 356 nm.

The electrooxidation of RR2 at the carbon felt causes changes of absorbance values which are similar to changes observed during the dye electrooxidation at the Ti/TiO_2(70%)–RuO_2(30%) electrode. The absorbance values decrease within the visible range if the anode potential increases up to 0.9 V. Further increase in the electrooxidation potential does not affect absorbances. Within the near ultraviolet region, the values of absorbances are almost the same. The highest conversion of the dye calculated as the change in TOC and COD was obtained at the potential of 1.0 V and totals 8 and 28%, respectively. This corresponds to a decrease in TOC and COD values in absolute terms from 68.3 ppm and 172.3 mg L^{-1} (RR2 initial solution) to 62.6 ppm and 123.5 mg L^{-1}, respectively.

3.3 Radiolysis

Radiolysis of water is a convenient way of producing defined amounts of radicals:

$$H_2O \rightsquigarrow e_{aq}^-, {}^\bullet H, {}^\bullet OH \quad (1)$$

In N_2O-saturated solution, e_{aq}^- is quantitatively converted into $^\bullet OH$ radical:

$$e_{aq}^- + N_2O + H_2O \rightarrow {}^\bullet OH + N_2 + OH^- \quad (2)$$

so that the yield of $^\bullet OH$ per 100 eV absorbed radiation, G(OH), is equal to 6.0 [39]. Since G(H) = 0.56, in irradiated N_2O-saturated aqueous solutions, the $^\bullet OH$ radicals constitutes more than 90% of all the radicals produced.

Experiments of pulse radiolysis were carried out in order to determine intermediate products of the reaction with $^\bullet OH$ radicals. The primary reactions of $^\bullet OH$ radicals with dyes molecules were investigated by 17 ns pulse radiolysis. The transient absorption spectra of N_2O-saturated aqueous solutions of RR2 (8×10^{-5} mol L^{-1}) and RB81 (6×10^{-5} mol L^{-1}) obtained at time scale of microseconds are presented in Figs. 6 and 7.

In transient spectra produced by the reaction of $^\bullet OH$ radicals with both dyes, shown in Figs. 6 and 7, the Δabsorbance is the difference in absorbance between the irradiated solution and the unirradiated one, taken at given time intervals after the pulse. The negative absorption

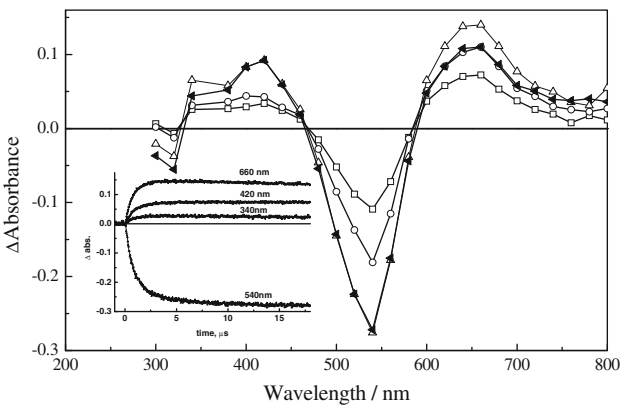

Fig. 6 Difference absorption spectra of transients following pulse radiolysis of N_2O saturated RR2 solution (8×10^{-5} mol L^{-1}) taken at 0.5 μs (-□-), 1.0 μs (-○-), 10.0 μs (-△-) and 70.0 μs (-◀-) after the 17 ns pulse (dose 55 Gy). *Inset* Oscilloscope traces of absorbance recorded at 340, 420, 540 and 660 nm

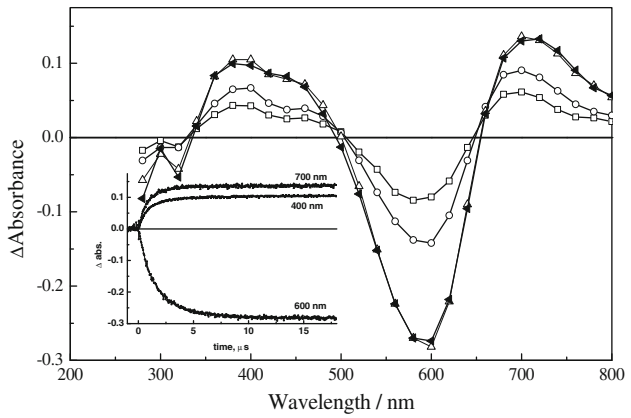

Fig. 7 Difference absorption spectra of transients following pulse radiolysis of N_2O saturated RB81 solution (8×10^{-5} mol L^{-1}) taken at 0.5 μs (-□-), 1.0 μs (-○-), 10.0 μs (-△-) and 70.0 μs (-◀-) after the 17 ns pulse (dose 55 Gy). *Inset* Oscilloscope traces of absorbance recorded at 400, 600 and 700 nm

bands are observed in the wavelength range where an intensive absorbance in unirradiated sample is exhibited and is caused by fading. In the transient spectra of both dyes one can observe two wavelength regions where negative Δabsorbance was recorded: at $\lambda < 330$ nm and in the visible range at 470–580 and 500–650 nm for RR2 and RB81, respectively. The positive value of Δabsorbance is obtained when the absorbance of the intermediate formed during and after the pulse is higher than the absorbance of unirradiated dye solution.

The hydroxyl radical can react with RR2 and RB81 by hydrogen abstraction or by addition to various parts of the dye molecule with diffusion-limited rate coefficients. The most probable position of the •OH addition is an aromatic ring in several positions (*ortho*-, *meta*-, *para*-) or the azo group in the dye molecule [35]. Therefore, the observed spectra are composite ones. The •OH addition to the azo chromophoric group leads to the destruction of the extensive conjugation and the intensive absorption band in the visible range disappears. The addition of •OH radical to a triazine ring is less probable due to smaller reactivity of this ring with the radical and the fact that rate of this reaction is slow [36, 37]. At the same time, the absorption bands in the wavelength range from 330 to 470 nm observed in the spectra recorded in the RR2 solution (Fig. 6) as well as in the wavelength range from 330 to 500 nm in the RB81 solution (Fig. 7) result from the •OH addition to the aromatic ring in the dye molecule. This is due to the fact that cyclohexadienyl and naphthoxyl-type radicals show typical absorbance bands in the wavelengths between 300 and 400 nm [35, 38].

The cyclohexadienyl radical can react with other cyclohexadienyl radicals by disproportionation or/and dimerization. The dimer generated via recombination of two cyclohexadienyl radicals may not have the conjugated colour giving part when it consists of two cyclohexadiene rings. The radical disproportionation leads to compounds that contain cyclohexadiene ring and another compound with extensive conjugation in the molecule characteristic to the dye and with an additional OH group [36, 39].

The oxidizing degradation of RR2 and RB81 by •OH radicals, in a long time range, was investigated in the steady-state radiolysis measurements. The influence of the dose on the absorption spectrum of RR2 and RB81 is shown in Fig. 8. In the upper part (B and D) of both figures the influence of the dose on difference spectra is presented in order to find common links between the pulse radiolysis and stationary irradiation data.

The UV bands in the range of 280–320 nm and visible bands of both dyes disappeared with an increase in dose. At the same time, formation of a very wide absorption band in the range of 340–450 and 350–480 nm for RR2 and RB81, respectively, can be observed. The latter absorption bands can be ascribed to the products of reactions of cyclohexadienyl radicals which contain cyclohexadiene rings. The absorption band recorded during radiation-induced discolouration of RR2 (Fig. 8) at wavelength range above 570 nm can be assigned to dye molecule containing an extra OH group in the conjugated part of the molecule as it was suggested by Wojnarovits et al. [35]. The visible bands of both dyes can be decreased to the minimum value for doses in the range 15–16 kGy (inset in Fig. 8A, C).

Results of quantum-chemical calculations were used in the estimation of the most probable position of the hydroxyl radical addition to the molecule of RR2 and RB81. The stabilities of radical adducts were assessed taking into consideration formation enthalpies of radical adducts calculated by the AM1 method (Table 2).

The calculated enthalpies of radical adducts formation in all positions of the benzene and naphthalene ring in the RR2 and RB81 molecule prove that the most stable adducts are formed by the radical hydroxylation of the naphthalene ring at the azo group in both dyes. The most probable position of hydroxylation seems to be C8 in both dyes.

3.4 Possible reaction pathways of reactive dyes electrochemical degradation

Intermediate products formed in the first step of reactive dyes electrooxidation and during "deep" oxidation were identified by GC–MS analysis. The solutions of RR2 and RB81 after electrolyses under potentiostatic conditions in the potential range from 0.6 to 2.0 V and at the electrical charge corresponding to the transfer of two electrons, were analyzed. Products of "deep" electrooxidation under galvanostatic conditions, obtained during 2 h electrolyses at

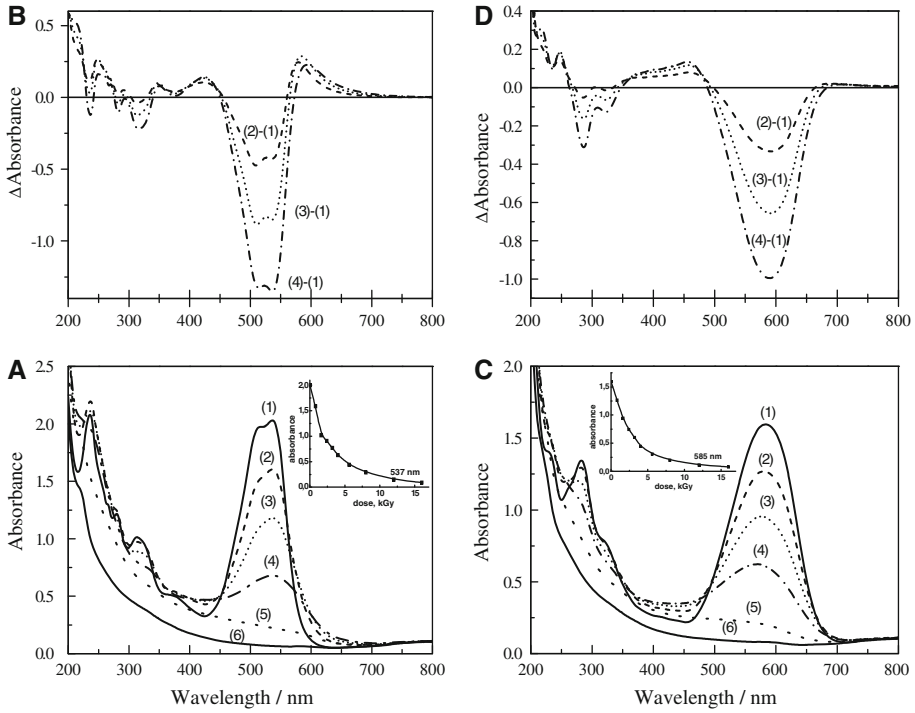

Fig. 8 Influence of dose on the absorption spectrum of RR2—7×10^{-5} mol L^{-1} (**A**) and RB81—6×10^{-5} mol L^{-1} (**C**) in N_2O saturated solution: (*1*) before irradiation, (*2*) 0.8 kGy, (*3*) 1.6 kGy, (*4*) 3.2 kGy, (*5*) 8 kGy and (*6*) 16 kGy. The dose of 0.8 kGy was obtained during a single pulse (4 μs). *Insets* Influence of dose on absorbance recorded at 537 nm (RR2) and 585 nm (RB81). Difference spectra of RR2 (**B**) and RB81 (**D**) obtained by subtraction of optical spectrum of non-irradiated sample (*1*) from spectrum of sample irradiated with appropriate dose indicated in part (A-RR2 or C-RB81)

Table 2 Stability of possible adducts of RR2 with hydroxyl radical calculated with AM1 method

Position of atom	Enthalpy of formation (kcal mol^{-1})	
	RR2	RB81
1	−118.7	−206.0
2	−122.1	−213.6
3	−113.4	−199.4
4	−128.9	−214.4
5	−126.2	−214.5
6	−119.8	−199.2
7	−113.5	−206.3
8	−138.9	−222.0
9	−108.3	−194.3
10	−105.9	−190.9
11	−97.2	−182.4
12	−90.6	−175.7
13	−113.5	−216.9
14	−121.5	−217.8
15	−121.8	−197.5
16	−126.2	−194.8
17	−124.4	−211.5
18	−126.0	−210.3
19	–	−199.8
20	–	−211.1
21	–	−210.3
22	–	−213.1
23	–	−208.4
24	–	−209.4

the current intensity of 0.4 A (i = 0.02 A cm^{-2}) were also investigated.

Figure 9 presents GC–MS chromatograms recorded in the initial solution of RR2 and in the dye solutions containing intermediates after the electrooxidation at the potential of 0.7 and 1.5 V. Comparison of these chromatograms shows only a decrease in the intensity of peaks at various retention times and lack of new peaks in the case of electrolyses carried out at lower potentials, i.e., below 1.0 V (Fig. 9A, B). This fact proves separation of one electron and addition of $^{\bullet}$OH radical to the dye molecule taking place in the first step of the electrooxidation. A similar dependence was observed in the first step of the RB81 electrooxidation.

Addition of $^{\bullet}$OH radical to the dye molecule, especially to naphthalene ring, and formation of naphtoxyl-type radical was confirmed by the pulse radiolysis experiments and calculations of radical adducts stability.

The next steps of the dyes electrooxidation and formation of new intermediates (Fig. 9C; Table 3) were observed during electrolyses at higher potentials (1.5 and 2.0 V) and higher electrical charge (890 C). Moreover, some peaks characteristic for the initial dye solution, e.g., peaks at the retention time of 3.6, 4.0, 19.6 and 20.3 s, disappeared. Similar compounds were identified during the analysis of the RB81 solutions after the electrooxidation at higher potentials.

Degradation of the dyes under galvanostatic conditions causes significant mineralization which results in the formation of substituted benzene rings, carboxylic acids and

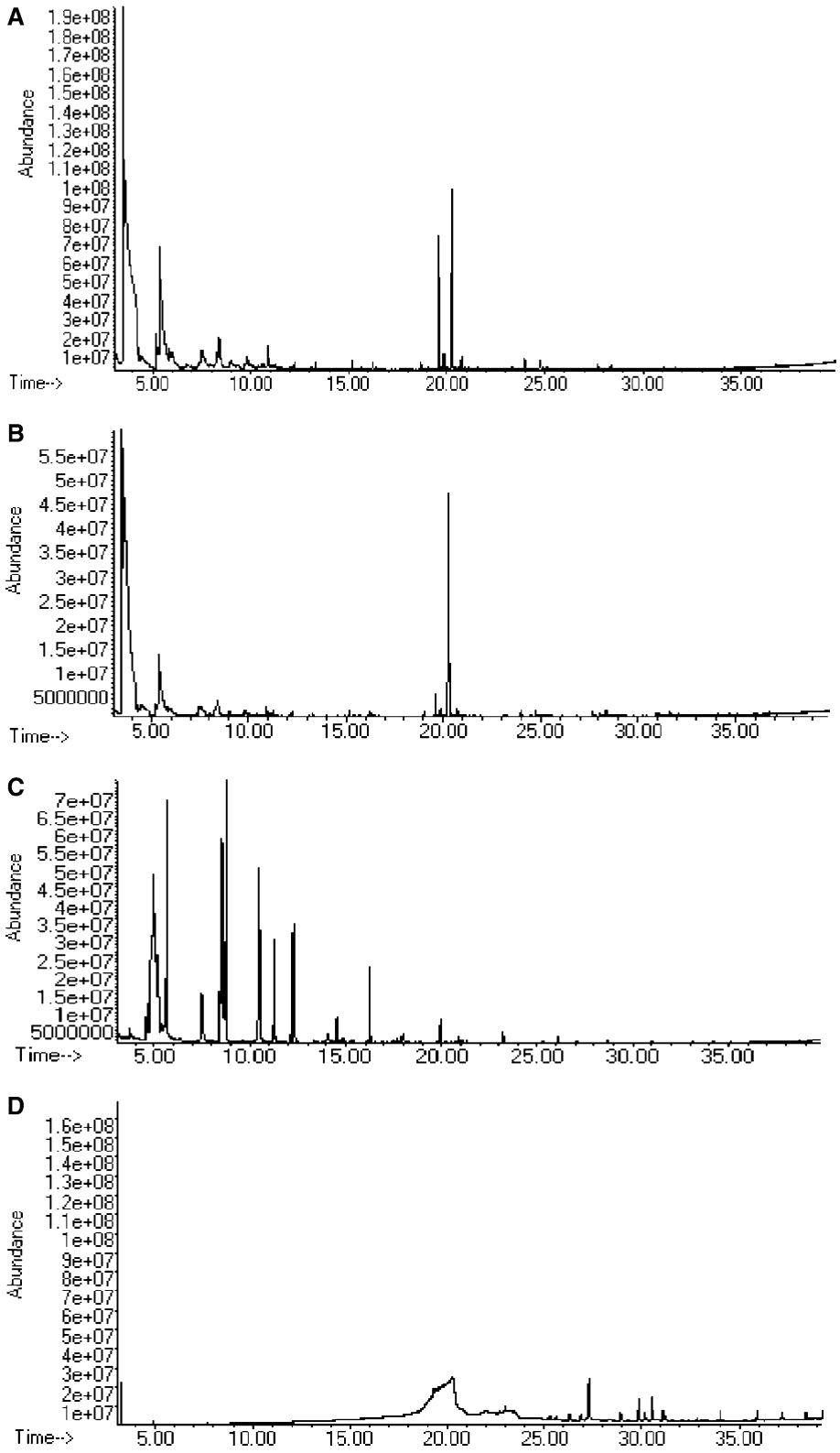

Fig. 9 GC/MS chromatograms recorded in the solution of RR2 before electrooxidation (**A**), after electrooxidation at 0.7 V (**B**), 1.5 V (**C**) and under galvanostatic conditions (**D**)

hydrocarbons (Fig. 9D; Table 3). Degradation of the RB81 dye is easier and results in one peak in the GC–MS chromatogram ($t_r = 34$ min, $C_{18}H_{38}$, $M_w = 254$). This peak corresponds to aliphatic carboxylic acids.

Results of voltammetric, pulse radiolysis measurements and electrolyses products identified by the GC–MS method suggest two possible pathways of the reactive dyes degradation. These pathways for the RR2 degradation are

Table 3 Degradation products of RR2 electrooxidation

Retention time (min)	Possible organic compound	Formula	m/z
Electrolysis 1.5 V			
10.47	2-Propenoic acid, 3-(3,4-dimethoxyphenyl)-	$C_{11}H_{12}O_4$	208
11.27	3(2H)-Benzofuranon,6-metoxy-2-[(4-methoxyphenyl)methylene]-	$C_{17}H_{14}O_4$	282
16.26	4H-1-Benzopyran-4-one, 3,5,7-trimethoxy-2-(4-methoxyphenyl)-	$C_{19}H_{18}O_6$	342
Electrolysis 2.0 V			
8.69	3(2H)-Benzofuranon,6-metoxy-2-[(4-methoxyphenyl)methylene]-	$C_{17}H_{14}O_4$	282
10.41	1,2-Benzenodiol (1,4-benzenodiol)	$C_{14}H_{22}O_2$	222
11.26	3(2H)-Benzofuranon,6-metoxy-2-[(4-methoxyphenyl)methylene]-	$C_{17}H_{14}O_4$	282
12.25	4H-1-Benzopyran-4-one, 3,5,7-trimethoxy-2-(4-methoxyphenyl)-	$C_{19}H_{18}O_6$	342
14.12	3(2H)-Benzofuranon,6-metoxy-2-[(4-methoxyphenyl)methylene]-	$C_{17}H_{14}O_4$	282
16.26	4H-1-Benzopyran-4-one, 3,5,7-trimethoxy-2-(4-methoxyphenyl)-	$C_{19}H_{18}O_6$	342
Electrolysis—"deep" oxidation			
19.33	1,2,4-Benzenotriol	$C_6H_6O_6$	126
20.00	Undecanoic acid	$C_{11}H_{22}O_2$	186
27.31	n-Hexadecanoic acid	$C_{16}H_{32}O_2$	256
30.15	Oleic acid	$C_{18}H_{34}O_2$	282
30.54	Octadecanoic acid	$C_{18}H_{36}O_2$	284
31.10	1-Hexadecanol, 2-methyl-	$C_{17}H_{36}O$	256

presented in Figs. 10 and 11. Electrochemical degradation of the dyes can proceed by direct electrooxidation or indirectly by oxidation with $^{\bullet}$OH radicals formed in this process. In the first step of the reactive dye degradation, formation of the dye cation-radical (Fig. 10) or addition of the $^{\bullet}$OH radical to the dye molecule (Fig. 11) takes place. The dye cation-radical can attach the $^{\bullet}$OH radical or can undergo oxidation with formation of a proper naphthoquinone derivative. If the $^{\bullet}$OH radical is attached to the carbon atom at the azo bond in the dye molecule, then the azo bond is cleaved. Further oxidation with $^{\bullet}$OH radicals results in the formation of appropriate quinones, naphthoquinones and benzenofuranes. Subsequent steps of the process lead to the formation of carboxylic acids and total mineralization of the dye is observed. The azo bond cleavage proceeds during the electrolyses at the potentials higher than 1.5 V and higher electrical charges. Higher mineralization of the dye solution was achieved during the 2 h electrolysis at the current density of 0.02 A cm^{-2}. Almost total mineralization can be achieved in photoelectrocatalytic process at the Ti/TiO_2(70%)–RuO_2(30%) electrode (i = 0.02 A cm^{-2}) with an application of radiation at the wavelength of 254 nm.

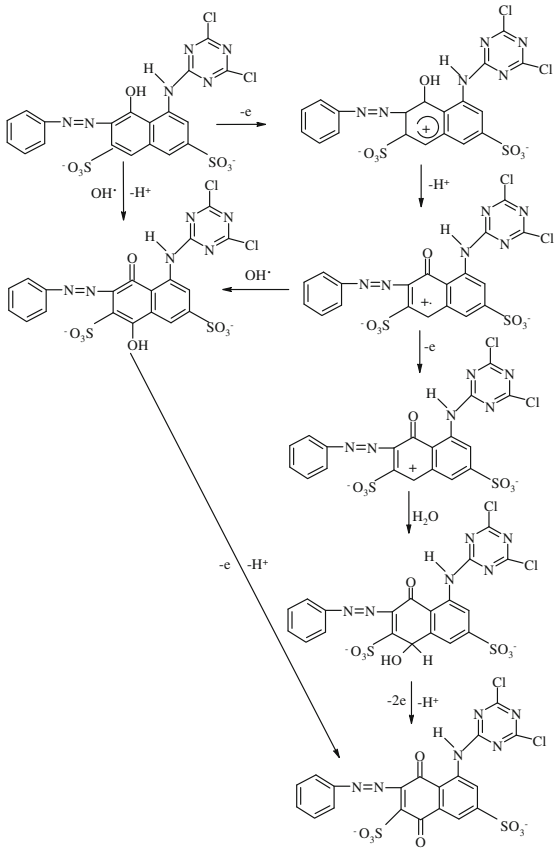

Fig. 10 Possible pathway of RR2 degradation during the electrochemical oxidation at the potentials lower than the potential at which oxygen evolution starts

4 Conclusions

Results of voltammetric investigations show that RR2 and RB81 is oxidised irreversibly in at least one electrode step

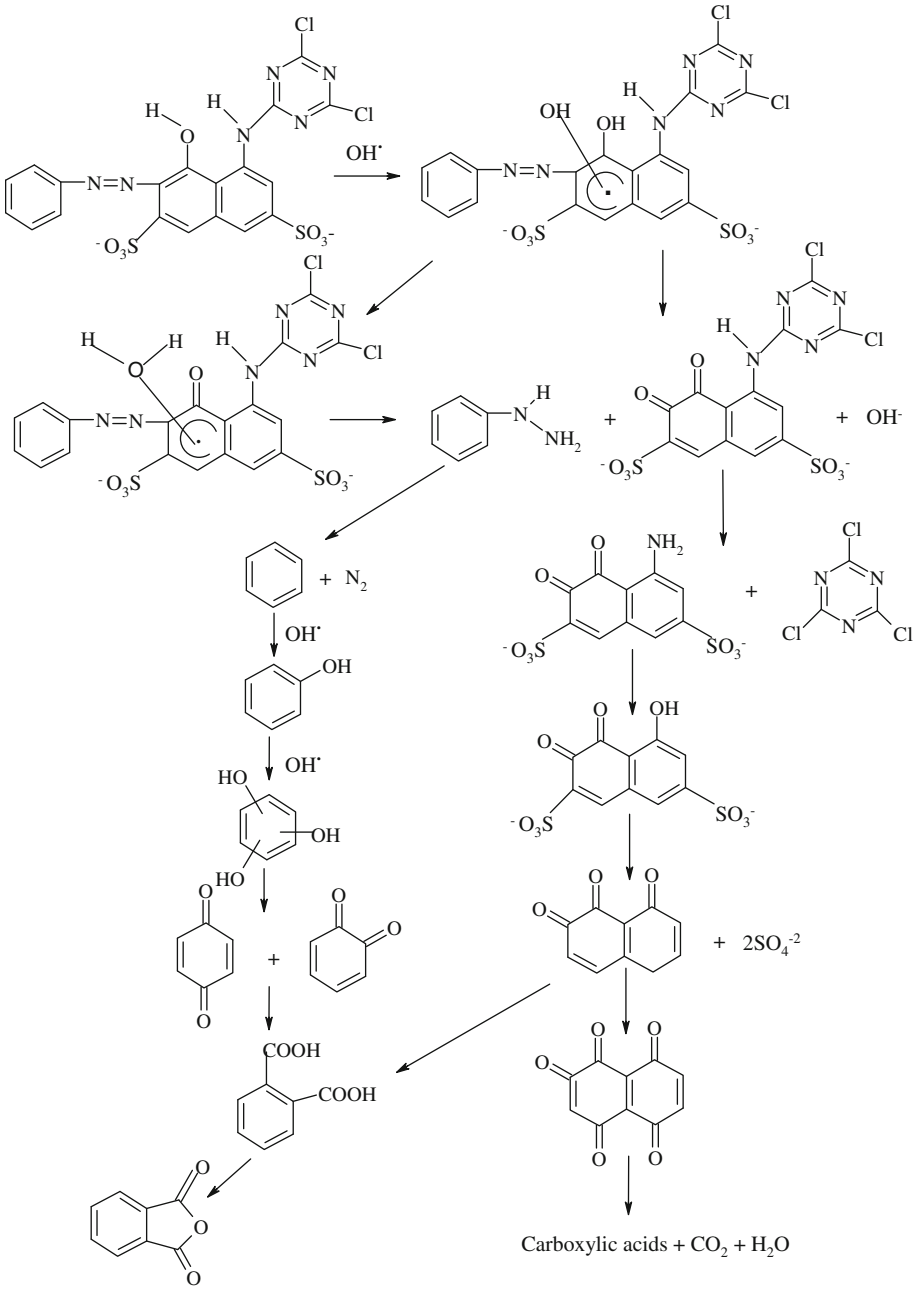

Fig. 11 Possible pathway of RR2 degradation by hydroxyl radicals

in the potential range lower than the potential at which oxygen evolution starts at the applied electrodes. Results of voltammetric measurements show that the electrooxidation of both dyes proceeds easier and with higher rate at $Ti/TiO_2(70\%)–RuO_2(30\%)$ than at carbon felt electrode.

The electrooxidation of RR2 under potentiostatic conditions results in better effectiveness if the $Ti/TiO_2(70\%)–RuO_2(30\%)$ electrode is applied. Then the highest conversion of the dye (14%), calculated as the change in TOC value, is achieved at the potential of 0.9 V. Lower conversion of RR2 (8%) is achieved at the carbon felt electrode and at the potential of 1.0 V. This electrode material can be partially destructed at potentials higher than 0.9 V which results in a very low decrease of TOC value. In the case of RB81 electrooxidation better results were obtained at the carbon felt. The TOC decrease was about 20% at the potential of 0.8 V but at this potential destruction of the carbon felt was not observed.

Changes in UV–VIS spectra recorded during pulse and steady-state radiolysis experiments prove the addition of $^{\bullet}OH$ radical to the aromatic ring in the dye molecule due to the fact that cyclohexadienyl and naphthoxyl-type radicals show typical absorbance bands in the wavelengths between 300 and 400 nm. Results of steady-state radiolysis

measurements show formation of the new absorption band above 570 nm which can be assigned to the dye molecule containing extra OH group in the conjugated part of the molecule.

Quantum-chemical calculations of the radical adducts stabilities confirmed the possibility of radical hydroxylation of the naphthalene ring at the azo group in both dyes.

GC–MS analysis of the intermediate products formed in the first step of reactive dyes electrooxidation under potentiostatic conditions and during "deep" electrooxidation as well as results of voltammetric and pulse radiolysis experiments, suggest two possible pathways of the dyes degradation. The first step of the dyes electrooxidation includes formation of the dye cation-radical or addition of $^{\bullet}$OH radical to the dye molecule resulting in the formation of a proper naphthoquinone derivative or the azo bond cleavage. At higher anode potentials and with higher electrical charges, formation of carboxylic acids and higher mineralization of the dye is observed.

References

1. Shaul GM, Holdsworth TJ, Dempsey CR, Dostall KA (1991) Chemosphere 22:107
2. Swamy J, Ramsay JA (1999) Enzyme Microb Technol 24:130
3. Kudlich M, Bishop PL, Knackmuss HJ, Stolz A (1996) Appl Microbiol Biotechnol 46:597
4. Koparal AS, Yavuz Y, Gürel C, Öguteveren ÜB (2007) J Hazard Mater 145:100
5. Mahmoodi NM, Arami M (2009) J Photochem Photobiol B 94:20
6. Fan L, Zhou Y, Yang W, Chen G, Yang F (2008) Dyes Pigment 76:440
7. Janssen LJJ, Koene L (2002) Chem Eng J 85:137
8. Jüttner K, Galla U, Schmieder H (2000) Electrochim Acta 45:2575
9. Fernandes A, Morão A, Maringho M, Lopes A, Gonçalves I (2004) Dyes Pigment 61:287
10. Johnsson DC, Feng J, Houk LL (2000) Electrochim Acta 46:323
11. Sakalis A, Fytianos K, Nickel U, Voulgaropoulos A (2006) Chem Eng J 119:127
12. Panizza M, Bocca C, Cerisola G (2000) Water Res 34:2601
13. Shen ZM, Wu D, Yang J, Yuan T, Wang WH, Jia JP (2006) J Hazard Mater 131:90
14. Carneiro PA, Osugi ME, Fugivara CS, Boralle N, Furlan M, Zanoni MVB (2005) Chemosphere 59:431
15. Rodrignez J, Rodrigo MA, Panizza M (2009) J Appl Electrochem 39:2285
16. Chen X, Gao F, Chen G (2005) J Appl Electrochem 35:185
17. Galindo C, Jacques P, Kalt A (2001) J Photochem Photobiol A Chem 141:47
18. Jain R, Sharma N, Radhapyari K (2009) J Appl Electrochem 39:577
19. Oliviera FH, Osagi ME, Paschoal FMM, Profeti D, Olivi P, Zanoni MVB (2007) J Appl Electrochem 37:583
20. Li X, Cui Y, Feng Y, Xie Z, Gu J (2005) Water Res 39:1972
21. Kesselman JM, Weres O, Lewis NS, Hoffmann MR (1997) J Phys Chem B 101:2637
22. Carneiro PA, Osugi ME, Sene JJ, Anderson MA, Zanoni MVB (2004) Electrochim Acta 49:3807
23. Wu M, Zhao G, Li M, Liu LL, Li D (2009) J Hazard Mater 163:26
24. Zanoni MVB, Sene JJ, Anderson MA (2003) J Photochem Photobiol A Chem 157:55
25. Candal RJ, Zeltner WA, Anderson MA (2003) Environ Sci Technol 34:3443
26. Kim DH, Anderson MA (1994) Environ Sci Technol 28:479
27. Osugi ME, Rjeshwar K, Ferraz ERA, Oliveira DP, Araujo AR, Zanoni MVB (2009) Electrochim Acta 54:2086
28. Camp R, Sturrock PE (1990) Water Res 24:1275
29. Pierce J (1994) J Soc Dyers Colour 110:131
30. Fan L, Yang F, Yang W (2004) Sep Purif Technol 34:89
31. Karolczak S, Hodyr K, Polowinski M (1992) Radiat Phys Chem 39:1
32. Chrzescijanska E, Kusmierek E, Nawrat G (2009) Pol J Chem 83:1115
33. Feng W, Nansheng D, Helin H (2000) Chemosphere 41:1233
34. Brahmia O, Richard C (2003) J Photochem Photobiol A Chem 156:9
35. Wojnarovits L, Palfi T, Takacs E (2007) Radiat Phys Chem 76:1497
36. Karpel N, Leitner V, Berger P, Gehringer P (1999) Radiat Phys Chem 55:317
37. Wojnarovits L, Palfi T, Takacs E, Emmi SS (2005) Radiat Phys Chem 74:239
38. Wojnarovits L, Takacs E (2008) Radiat Phys Chem 77:225
39. Klein G, Schuler RH (1978) Radiat Phys Chem 11:167